Biophysical Chemistry 219 (2016) 43–48

Contents lists available at ScienceDirect

Biophysical Chemistry

journal homepage: http://www.elsevier.com/locate/biophyschem

# Molecular dynamics of the honey bee toxin tertiapin binding to Kir3.2

Daxu Li [a], Rong Chen [b,*], Shin-Ho Chung [b]

[a] College of Medicine, Xi'an Jiaotong University, Xi'an 710061, China
[b] Research School of Biology, Australian National University, Acton, ACT 2601, Australia

## HIGHLIGHTS

- Tertiapin blocks Kir3.2 by inserting the Lys17 side chain into the channel pore
- Glu127 of Kir3.2 is important for tertiapin selectivity.
- PMF calculations can help identify the most favorable binding mode.

## GRAPHICAL ABSTRACT

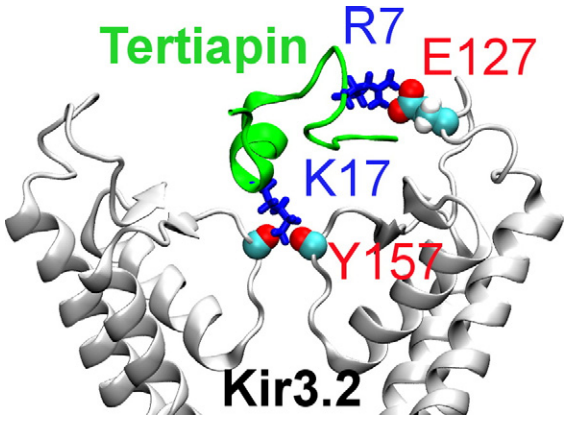


## ARTICLE INFO

*Article history:*
Received 3 June 2016
Received in revised form 29 August 2016
Accepted 29 September 2016
Available online 30 September 2016

*Keywords:*
Kir3.2
Tertiapin
Molecular dynamics
Honey bee toxin

## ABSTRACT

Tertiapin (TPN), a short peptide isolated from the venom of the honey bee, is a potent and selective blocker of the inward rectifier $K^+$ (Kir) channel Kir3.2. Here we examine in atomic detail the binding mode of TPN to Kir3.2 using molecular dynamics, and deduce the key residue in Kir3.2 responsible for TPN selectivity. The binding of TPN to Kir3.2 is stable when the side chain of either Lys16 ($TPN^{K16}$-Kir3.2) or Lys17 ($TPN^{K17}$-Kir3.2) of the toxin protrudes into the channel pore. However, the binding affinity calculated from only $TPN^{K17}$-Kir3.2 and not $TPN^{K16}$-Kir3.2 is consistent with experiment, suggesting that Lys17 is the most plausible pore-blocking residue. The alanine mutation of Kir3.2-Glu127, which is not present in TPN-resistant channels, reduces the inhibitory ability of TPN by over 50 fold in $TPN^{K17}$-Kir3.2, indicating that Kir3.2-Glu127 is important for the selectivity of TPN.



## 1. Introduction

Inward rectifier $K^+$ (Kir) channels help establish the resting membrane potential of excitable cells by allowing the flow of $K^+$ ions into the cell. They are involved in many physiological processes and implicated in a number of diseases such as the Andersen syndrome and cardiac disorders [1]. Several Kir channels such as Kir1.1 and Kir6.2 are potential drug targets [2].

Tertiapin (TPN), a peptide composed of 21 amino acids isolated from the venom of honey bee, is a potent inhibitor of several Kir channel isoforms such as rat Kir1.1 and mouse Kir3.2 [3]. Solution structure of TPN shows that the backbone of the toxin is interconnected by two disulfide bonds, thereby conferring structural rigidity [4]. The toxin carries four lysine residues all of which are from the α-helix near the C-terminus (Fig. 1A).

* Corresponding author.
*E-mail address:* rong.chen@anu.edu.au (R. Chen).

http://dx.doi.org/10.1016/j.bpc.2016.09.010
0301-4622/

Crystal structures of several isoforms of Kir channels have shown that the transmembrane pore domain is similar to that of other families of $K^+$ channels such as the voltage-gated $K^+$ (Kv) channel [5–8]. Several rings of acidic residues on the outer vestibule of Kir3.2 (Fig. 1B) may interact favorably with the positively charged TPN. It is thus plausible that TPN blocks Kir3.2 by inserting one of its lysine residues to the channel filter, in a way similar to that demonstrated for scorpion toxins and Kv channels [9]. Mutagenesis experiments performed on TPN showed that the mutation of each of the four lysine residues causes similar reduction (5–20 fold) in toxin affinity [10]. Therefore, available experimental data are not conclusive as to which lysine of TPN is the pore-blocking residue.

TPN is specific for certain Kir isoforms. Some Kir channels such as the human Kir1.1 are resistant to TPN (Fig. 1C). Thus, it is of interest to understand the structural basis of TPN inhibition and specificity, to be able to design TPN variants specific for different Kir channels. A number of computational studies focusing on understanding the binding mode of TPN to Kir channels have been reported [11–14]. In all these studies a rigid-body docking method was used to predict the binding modes of the toxin to the channel. A limitation of rigid-body docking is that the prediction is sensitive to the conformation of the ligand and receptor. Therefore, divergent models of toxin-channel complexes have been proposed in these studies, in which different toxin structures and channel models were used. For example, the 12th conformer of the 21 solution structures of TPN was proposed to be in the best conformation to interact with rKir1.1 [14]. The Lys17 residue of TPN was predicted to be the pore-blocking residue for Kir3.2 [11], whereas different pore-blocking residues (His12 and Lys21) were proposed for Kir1.1 [12–14]. Whether TPN can block Kir3.2 or Kir1.1 with multiple pore-blocking residues is unclear, although a multiple-binding-mode mechanism has been demonstrated for μ-conotoxins and $Na^+$ channels [15,16].

Here we perform a systematic search to identify the pore-blocking residue of TPN for Kir3.2 using molecular dynamics (MD). To avoid the limitations of rigid-body docking, MD simulations with distance restraints, in which both toxin and channel are flexible, are used to predict TPN-Kir3.2 complex structures. All the four possible binding modes of TPN-Kir3.2 in which each of the four lysine residues (Lys16, Lys17, Lys20 and Lys21) of the toxin occludes the pore of the channel are constructed. The binding mode in which Lys17 protrudes into the pore ($TPN^{K17}$-Kir3.2) reproduces the binding affinity of TPN to Kir3.2 measured experimentally. On the other hand, all other binding modes are either unstable ($TPN^{K20}$-Kir3.2 and $TPN^{K21}$-Kir3.2) or of much lower binding affinity (1.2 μM, $TPN^{K16}$-Kir3.2), indicating that $TPN^{K17}$-Kir3.2 is the most plausible binding mode. In the $TPN^{K17}$-Kir3.2 complex, Kir3.2-Glu127 makes a salt bridge with TPN-Arg7. Our calculations show that the alanine mutation of Kir3.2-Glu127 reduces the binding affinity of TPN by about 50 fold, suggesting that Kir3.2-Glu127 may be crucial for the high-affinity binding and selectivity of TPN.

## 2. Methods

### 2.1. Starting configuration

The pore domain (residues 89 to 196) of the crystal structure of Kir3.2 (PDB ID 3SYA [6]) is embedded in a POPC (1-palmitoyl-2-oleoyl-*sn*-glycero-3-phosphocholine) bilayer and a box of explicit water. The simulation box, containing the Kir3.2 pore domain, 165 POPC lipids and 15,888 water molecules, is approximately 85 × 85 × 105 $Å^3$ in size. A total of 68 $K^+$ and 60 $Cl^-$ ions are added into the system to maintain charge neutrality and a salt concentration of 0.2 M. The system is equilibrated for 20 ns before TPN is added subsequently.

After the system is equilibrated, the last conformer of the solution structure of TPN (PDB ID 1TER [4]) is placed 15 Å above the position where the toxin is fully bound (Fig. 2). MD simulation with distance restraint, which has been successfully applied to many similar toxin-channel systems [17–19], is used to predict the binding mode of TPN to the channel. The advantage of this method over rigid-body docking is that

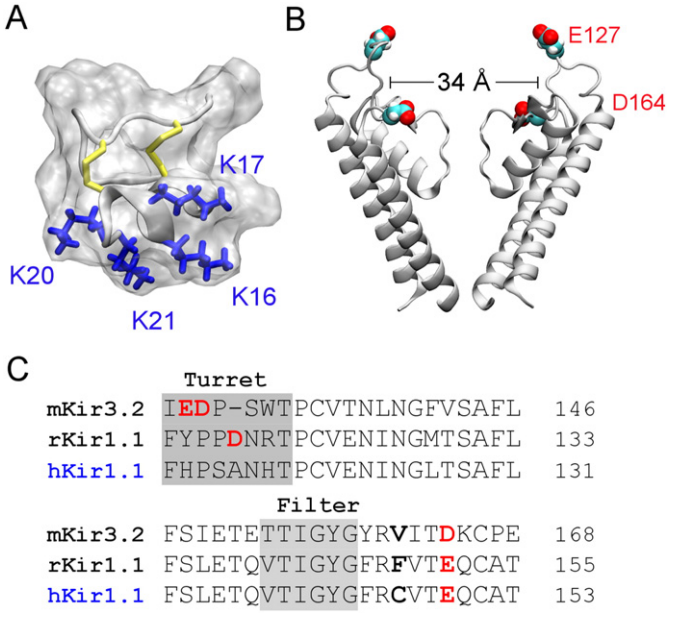


**Fig. 1.** Structure of TPN and Kir3.2. (A) Solution structure of TPN (PDB ID 1TER [4]). Two disulfide bonds are shown in yellow, and the side chains of four lysine residues in blue. (B) Crystal structure of mouse Kir3.2 (PDB ID 3SYA [6]). Only the transmembrane pore domain of two subunits is shown. The position of two acidic residues (Glu127 and Asp164) relative to the outer vestibule is highlighted. (C) Sequence alignment of three Kir channel isoforms, mouse Kir3.2 (mKir3.2), rat Kir1.1 (rKir1.1) and human Kir1.1 (hKir1.1). The hKir1.1 is relatively insensitive to TPN block.

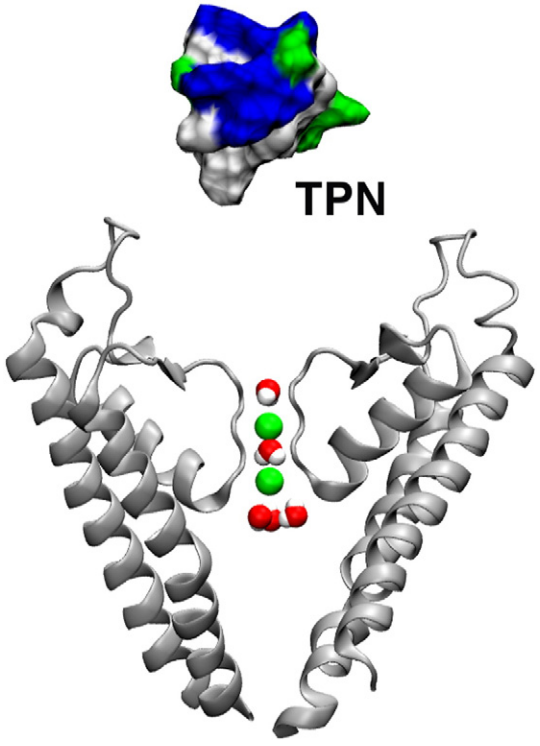


**Fig. 2.** The position of TPN relative to Kir3.2 at the start of the MD simulation. Several water molecules and two $K^+$ ions (green spheres) in the filter are shown. Basic residues of the toxin are colored in blue.

structural flexibility of proteins as well as the interactions due to water is taken into account naturally. In order to examine all the possible binding modes, four complexes in which each of the lysine residues act as the pore-blocking residue are predicted. Specifically, a flat-bottom harmonic distance restraint is applied between the side chain nitrogen atom of a toxin lysine and the carbonyl group of Kir3.2-Gly156. The toxin is oriented randomly with the lysine facing the outer wall of the channel before the distance restraint is applied. When the side chain of the lysine protrudes into the selectivity filter, the nitrogen atom of the side chain is 4 Å above the plane of the carbonyl groups of the glycine. Thus, the upper boundary of the distance restraint is progressively reduced from 15 Å to 3 Å over a simulation period of 16 ns, so that the side chain of the lysine is gradually drawn into the selectivity filter. The force constant of the distance restraint is set to 1 kcal/mol/Å$^2$. The backbone of TPN is maintained rigid in the first 10 ns, so that no significant conformational changes in TPN are induced by the distance restraint. The simulation is continued until 50 ns with the distance restraint removed, allowing the toxin-channel complex to evolve to a stable state spontaneously.

### 2.2. Molecular dynamics

All MD simulations are performed under periodic boundary conditions using NAMD 2.10 [20]. The CHARMM36 force fields and the TIP3P model for water are used to describe the interatomic interactions in the system [21–23]. The switch and cutoff distances for short-range interactions are set to 8.0 Å and 12.0 Å, respectively. The long-range electrostatic interactions are accounted for using the particle mesh Ewald method, with a maximum grid spacing of 1.0 Å. Bond lengths are maintained rigid with the SHAKE and SETTLE algorithms [24,25], allowing a time step of 2 fs to be used. The average temperature and pressure are maintained constant at 300 K and 1 atm by using the Langevin dynamics and the Nosé-Hoover Langevin Piston method [26], respectively. The pressure coupling is semiisotropic. Trajectories are saved every 20 ps for analysis.

### 2.3. PMF calculations

PMF profiles are constructed with the umbrella sampling method. The reaction coordinate is the center of mass (COM) distance between the toxin and channel backbones along the channel axis ($z$). The starting structures of the umbrella windows spaced at 0.5 Å intervals are generated by pulling the toxin along the $z$ axis, using a harmonic force constant of 15 kcal/mol/Å. During the pulling the backbone of the toxin is maintained rigid using harmonic restraint, and the toxin is free to move and rotate. The biasing potential of each umbrella window is set to 30 kcal/mol/Å$^2$. The COM of the channel backbone is at $z = 0$ Å. A flat-bottom harmonic restraint is applied to maintain the COM of the toxin backbone within a cylinder of 8 Å in radius centered on the channel axis. Each umbrella window is simulated for at least 8 ns to ensure good convergence. The $z$ coordinates of toxin COM are saved every 1 ps. The first 1 ns of each window is removed from data analysis. The formal link between the PMF profile and the dissociation constant, $K_d$, has been derived using different statistical mechanical methods [9,27,28]. The $K_d$ can be calculated from the PMF, $W(z)$, using the following equation:

$$K_d^{-1} = 1000\pi R^2 N_A \int_{z_{min}}^{z_{max}} \exp[-W(z)/kT]dz \quad (1)$$

where $\pi R^2$ is the cross-sectional area of the cylinder, $N_A$ is Avogadro's number, $z_{min}$ and $z_{max}$ are the $z$ positions of the toxin COM when the toxin is fully bound to the channel and in the bulk, respectively.

## 3. Results and discussion

### 3.1. Binding to Kir3.2

Pore-blocking peptide toxins of $K^+$ channels are known to occlude the channel permeation pathways via the side chain of a lysine residue [9,29]. On the other hand, no experimental evidence supporting arginine and histidine as pore-blocking residue has been reported. This is possibly because the side chains of arginine and histidine are too bulky for the pore, which is only 2.8 Å in diameter. Therefore, we only consider the four lysine residues of TPN as possible pore-blocking residues. We predict all the binding modes of TPN-Kir3.2 in which each lysine residue of TPN blocks the channel pore using MD simulations with distance restraints. The biasing restraint is applied only in the first 16 ns and then removed until the simulation is terminated at 50 ns as described in the Methods. The distance restraint has no effect on the rotational degrees of freedom of the toxin. Each simulation is replicated a second time with different toxin orientation, and consistent results are obtained in all cases.

Snapshots of the TPN-Kir3.2 complexes at 16 ns and at the end of each simulation are shown in Fig. 3. In the presence of the biasing restraint, the lysine residue protrudes into the channel filter and forms a hydrogen bond with the carbonyl group of Tyr157 in all the binding modes (Fig. 3A–D). However, once the restraint is removed, Lys16 and Lys17 remain protruded into the pore (Fig. 3E–F), but Lys20 and Lys21 are completely ejected from the pore (Fig. 3G–H). Thus, Lys20 and Lys21 of TPN are unlikely to be the pore-blocking residues for Kir3.2.

### 3.2. Two possible binding modes

Having excluded Lys20 and Lys21 as the pore-blocking residue, we examine in detail the binding modes TPN$^{K16}$-Kir3.2 and TPN$^{K17}$-Kir3.2, in which the side chains of Lys16 and Lys17 occlude the channel pore, respectively. In both binding modes the lysine residue forms hydrogen bonds with the carbonyl groups of Tyr157 in the filter, and Arg7 forms a salt bridge with Glu127 from the turret of the channel (Fig. 4A and B). The Arg7-Glu127 residue pair is stable and persistent in TPN$^{K17}$-Kir3.2 (Fig. 4C). On the other hand, this residue pair is largely broken in TPN$^{K16}$-Kir3.2. To further verify the stability of Arg7-Glu127 and capture the most stable state of TPN$^{K16}$-Kir3.2, the simulation is extended until 70 ns. The salt bridge is persistent over the last 10 ns, indicating that the most favorable conformation of TPN$^{K16}$-Kir3.2 is obtained (Fig. 4C).

### 3.3. Binding affinities of the two modes

To determine which of the two binding modes predicted from MD is more favorable than the other, we construct the PMF profiles for the two modes and derive the dissociation constant ($K_d$) of the toxin binding using umbrella sampling. The starting structure of each umbrella window is generated by pulling the toxin out from its bound position along the channel axis until it is in the bulk, approximately 25 Å above its fully bound position. The PMF profiles derived from the two binding modes are expected to be similar in the region near the bulk, where the toxin-channel interactions are not significantly influenced by the initial binding mode. A similar PMF profile is obtained when the umbrella sampling simulations were replicated a second time for TPN$^{K16}$-Kir3.2 (Fig. 5), indicating that the random error of the PMF is small.

As expected, the profiles for the two binding modes virtually overlap in the region where the toxin is >5 Å above its fully-bound position ($26 < z < 40$ Å, Fig. 5). However, due to differences in the region where the toxin is closely bound to the channel ($20 < z < 26$ Å), the well depths differ by approximately 5.8 $kT$. The well depths of both PMF profiles derived from TPN$^{K16}$-Kir3.2 are about $-15.2$ $kT$, corresponding to a $K_d$ value of 1.2 μM. In contrast, the well depth of the profile is $-21$ $kT$ for TPN$^{K17}$-Kir3.2, corresponding to a $K_d$ value of 7 nM.

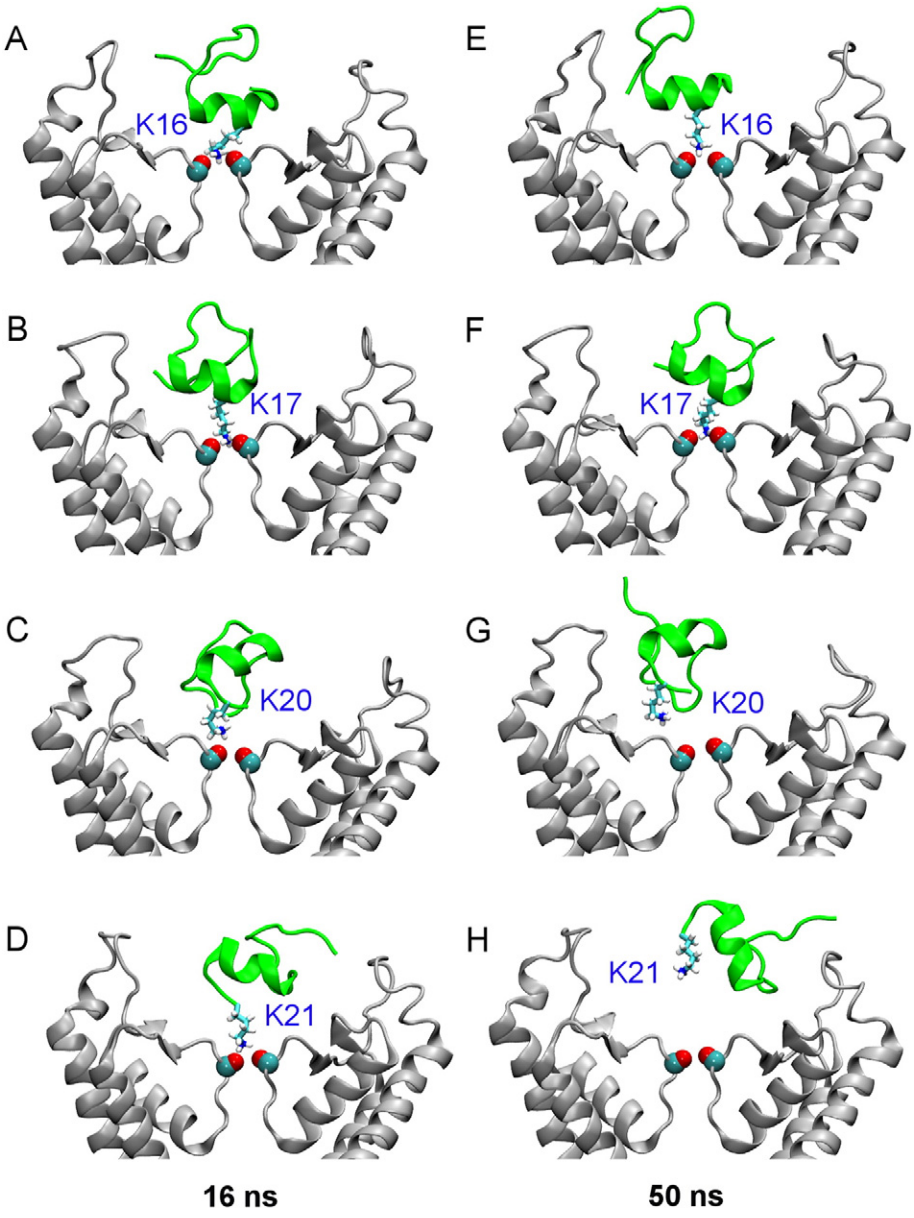


**Fig. 3.** The four complexes of TPN-Kir3.2 predicted from MD simulations. The binding mode at 16 ns when the biasing restraint is removed is shown on the left and at 50 ns when the simulation is terminated on the right. Toxin backbone is shown in green and channel backbone in white. Only two channel subunits are shown for clarity. Carbonyl groups of Tyr157 in the filter are shown as cyan and red spheres.

Experimentally the $K_d$ value of Kir3.2 block by TPN has been estimated to be 5–7 nM [30]. Thus, the $K_d$ value we computed from $TPN^{K17}$-Kir3.2 is in good agreement with experiment, indicating that Lys17 of TPN is the most plausible pore-blocking residue for Kir3.2.

### 3.4. Implications for TPN selectivity

In the most favorable TPN-Kir3.2 complex, $TPN^{K17}$-Kir3.2, two strong contacts are evident (Fig. 4B). In the first contact, the side chain of Lys17 protrudes into the filter, forming hydrogen bonds with backbone carbonyl groups of Tyr157. In the second contact, Arg7 of TPN forms strong electrostatic interactions with Glu127 from the turret. The selectivity filter region is highly conserved across $K^+$ channels including Kir channels. Thus, the first contact is unlikely the key determinant for toxin specificity. However, the second contact involves the turret region, which is much less conserved, and therefore, is more likely to be involved in toxin specificity.

The second contact predicts that an acidic residue from the channel turret is crucial for stabilizing the toxin-channel complex. This prediction is in excellent agreement with available experimental data, suggesting that our binding mode of $TPN^{K17}$-Kir3.2 is likely to be valid. For example, in the TPN-sensitive channel rKir1.1, an acidic residue equivalent to Glu127 of Kir3.2 is found at position 116 of its turret (Fig. 1C). Transferring the eleven residues in the turret of rKir1.1 to the TPN-resistant mKir2.1 ($IC_{50}$ 20 μM) transforms mKir2.1 into a TPN-sensitive channel ($IC_{50}$ 38 nM) [31]. The turret of the TPN-insensitive mKir2.1 channel carries two basic residues that would interact unfavorably with the positively-charged TPN. Similarly, in the TPN-insensitive channel hKir1.1, no equivalent acidic residue is present in the turret (Fig. 1C).

To verify the role of Kir3.2-Glu127 for TPN specificity, the $K_d$ value of TPN to the E127A mutant Kir3.2 is calculated. Specifically, starting from the bound $TPN^{K17}$-Kir3.2 complex, the side chain of Glu127 is replaced with that of an alanine, and a $K^+$ ion is removed from the bulk to maintain charge neutrality. The $TPN^{K17}$-[E127A]-Kir3.2 complex is then

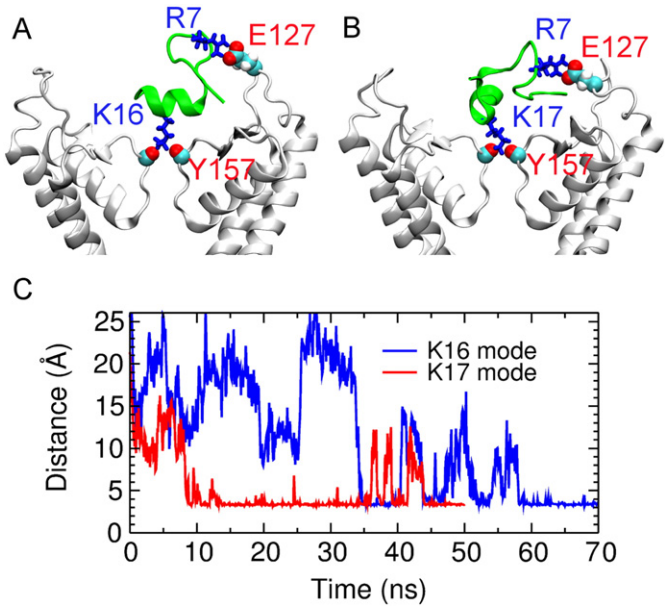


**Fig. 4.** Binding modes of TPN to Kir3.2 predicted from MD simulations. In (A) and (B), the two modes in which Lys16 and Lys17 occludes the filter are shown, respectively. In (C), the distance of the Arg7-Glu127 salt bridge as a function of simulation time is shown for $TPN^{K16}$-Kir3.2 (K16 mode) and $TPN^{K17}$-Kir3.2 (K17 mode).

equilibrated for 20 ns using molecular dynamics, and subsequently the PMF profile is derived from umbrella sampling simulations. The profile for the binding of TPN to the mutant channel shows a depth of −17.5 *kT*, corresponding to a $K_d$ value of 405 nM. Thus, the E127A mutation causes the binding affinity of TPN to reduce by approximately 58 fold, suggesting that Glu127 is important TPN binding and selectivity. This result is consistent with experiments, in which a 10-fold reduction in the inhibition effect of a TPN mutant, which is resistant to oxidation but otherwise functionally resembles the wild type, was observed after the E127A mutation to Kir3.2 [32].

## 4. Conclusions

MD simulations are used to examine the binding of a honey bee toxin, TPN, to the inward-rectifying $K^+$ channel, Kir3.2. TPN forms a stable complex with Kir3.2 only when Lys16 or Lys17 protrudes into the channel filter. However, PMF calculations indicate that the binding is approximately 5.8 *kT* more favorable when Lys17 is the pore-blocking residue. The $K_d$ value derived from complex in which Lys17 blocks the channel pore is in good agreement with those determined experimentally, indicating that the binding mode of TPN-Kir3.2 predicted from our simulations is likely to be valid. When Lys17 protrudes into the pore and forms a hydrogen bond with the carbonyl group of Tyr157, Arg7 of TPN forms a salt bridge with Glu127 from the channel turret. In a previous model of TPN-Kir3.2, Lys17 was also the pore-blocking residue, but the Arg7-Glu127 interaction was not present, which could account for the low $K_d$ value of 400 nM calculated [11]. Indeed, when Glu127 is mutated to an alanine, the $K_d$ value increases by >50 fold to 405 nM in our calculations. Thus, our results suggest that the lack of an acidic residue equivalent to Glu127 of Kir3.2 in the turrets of hKir1.1 and other TPN-insensitive channels may largely account for the TPN-resistance of these channels.

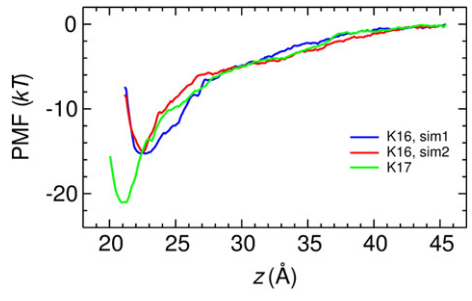


**Fig. 5.** PMF profiles of the binding of TPN to Kir3.2. The profiles are derived from the two binding modes, in which Lys16 and Lys17 protrudes into the channel filter, respectively. For the Lys16 binding mode, profiles from two independent sets of simulations (sim1 and sim2) are constructed.

Our results also demonstrate that the prediction of $K_d$ using PMF calculations is a reliable means of validating the complex structures predicted from MD. The starting configuration of each umbrella window is generated sequentially by pulling the toxin away from the bound position. Therefore, the orientation of the toxin is not random and the resulting PMF profile is biased, because the toxin would only explore a narrow configurational space over a limited period of simulation time. If the configurational space explored largely accounts for the partition function, the biased PMF profile would be similar to the true unbiased profile. Starting from the most favorable binding mode, it should be possible to sample the configurations that have the largest contributions to the partition function within a short period of simulation time and predict the experimental $K_d$ with reasonable accuracy. In the case of TPN-Kir3.2, the experimental $K_d$ value is reproduced only when Lys17 but not Lys16 is the pore-blocking residue, although both residues can stably block the pore, indicating that Lys17 is the most plausible pore-blocking residue. Thus, PMF calculations can help identify the most favorable binding mode when empirical properties such as the stability and number of hydrogen bonds are similar.

## Acknowledgements

All the calculations were undertaken on the National Computational Infrastructure in Canberra, Australia, which is supported by the Australian Commonwealth Government. This research was supported by the National Health and Medical Research Council of Australia (grant no. APP1070030) and the Medical Advances Without Animals Trust (MAWA).

## References

[1] H. Hibino, A. Inanobe, K. Furutani, S. Murakami, I. Findlay, Y. Kurachi, Inwardly rectifying potassium channels: their structure, function, and physiological roles, Physiol. Rev. 90 (2010) 291–366.
[2] G.J. Kaczorowski, O.B. McManus, B.T. Priest, M.L. Garcia, Ion channels as drug targets: the next GPCRs, J. Gen. Physiol. 131 (2008) 399–405.
[3] W. Jin, Z. Lu, A novel high-affinity inhibitor for inward-rectifier $K^+$ channels, Biochemistry 37 (1998) 13291–13299.
[4] X. Xu, J.W. Nelson, Solution structure of tertiapin determined using nuclear magnetic resonance and distance geometry, Proteins 17 (1993) 124–137.
[5] O.B. Clarke, A.T. Caputo, A.P. Hill, J.I. Vandenberg, B.J. Smith, J.M. Gulbis, Domain reorientation and rotation of an intracellular assembly regulate conduction in Kir potassium channels, Cell 141 (2010) 1018–1029.
[6] M.R. Whorton, R. MacKinnon, Crystal structure of the mammalian GIRK2 $K^+$ channel and gating regulation by G proteins, PIP2, and sodium, Cell 147 (2011) 199–208.
[7] M.R. Whorton, R. MacKinnon, X-ray structure of the mammalian GIRK2-βγ G-protein complex, Nature 498 (2013) 190–197.
[8] X. Tao, J.L. Avalos, J.Y. Chen, R. MacKinnon, Crystal structure of the eukaryotic strong inward-rectifier $K^+$ channel Kir2.2 at 3.1 Å resolution, Science 326 (2009) 1668–1674.
[9] D. Gordon, R. Chen, S.H. Chung, Computational methods of studying the binding of toxins from venomous animals to biological ion channels: theory and applications, Physiol. Rev. 93 (2013) 767–802.
[10] W. Jin, A.M. Klem, J.H. Lewis, Z. Lu, Mechanisms of inward-rectifier $K^+$ channel inhibition by tertiapin-Q, Biochemistry 38 (1999) 14294–14301.
[11] T.A. Hilder, S.H. Chung, Conductance properties of the inwardly rectifying channel, Kir3.2: molecular and Brownian dynamics study, Biochim. Biophys. Acta 2013 (1828) 471–478.
[12] T.A. Hilder, S.H. Chung, Conduction and block of inward rectifier $K^+$ channels: predicted structure of a potent blocker of Kir2.1, Biochemistry 52 (2013) 967–974.
[13] J. Hu, S. Qiu, F. Yang, Z.J. Cao, W.X. Li, Y.L. Wu, Unique mechanism of the interaction between honey bee toxin TPNQ and rKir1.1 potassium channel explored by computational simulations: insights into the relative insensitivity of channel towards animal toxins, PLoS One 8 (2013).

[14] C.A. Doupnik, K.C. Parra, W.C. Guida, A computational design approach for virtual screening of peptide interactions across $K^+$ channel families, Comput. Struct. Biotechnol. J. 13 (2015) 85–94.
[15] R. Chen, S.H. Chung, Binding modes of μ-conotoxin to the bacterial sodium channel ($Na_VAb$), Biophys. J. 102 (2012) 483–488.
[16] R. Chen, A. Robinson, S.H. Chung, Mechanism of μ-conotoxin PIIIA binding to the voltage-gated $Na^+$ channel $Na_V1.4$, PLoS One 9 (2014), e93267.
[17] R. Chen, S.H. Chung, Structural basis of the selective block of Kv1.2 by maurotoxin from computer simulations, PLoS One 7 (2012), e47253.
[18] M.A. Eriksson, B. Roux, Modeling the structure of agitoxin in complex with the *Shaker* $K^+$ channel: a computational approach based on experimental distance restraints extracted from thermodynamic mutant cycles, Biophys. J. 83 (2002) 2595–2609.
[19] R. Chen, S.H. Chung, Binding modes of two scorpion toxins to the voltage-gated potassium channel Kv1.3 revealed from molecular dynamics, Toxins 6 (2014) 2149–2161.
[20] J.C. Phillips, R. Braun, W. Wang, J. Gumbart, E. Tajkhorshid, E. Villa, C. Chipot, R.D. Skeel, L. Kalé, K. Schulten, Scalable molecular dynamics with NAMD, J. Comput. Chem. 26 (2005) 1781–1802.
[21] J.B. Klauda, R.M. Venable, J.A. Freites, J.W. O'Connor, D.J. Tobias, C. Mondragon-Ramirez, I. Vorobyov, A.D. MacKerell Jr., R.W. Pastor, Update of the CHARMM all-atom additive force field for lipids: validation on six lipid types, J. Phys. Chem. B 114 (2010) 7830–7843.
[22] A.D. MacKerell, D. Bashford, M. Bellott, R.L. Dunbrack, J.D. Evanseck, M.J. Field, S. Fischer, J. Gao, H. Guo, S. Ha, D. Joseph-McCarthy, L. Kuchnir, K. Kuczera, F.T.K. Lau, C. Mattos, S. Michnick, T. Ngo, D.T. Nguyen, B. Prodhom, W.E. Reiher, B. Roux, M. Schlenkrich, J.C. Smith, R. Stote, J. Straub, M. Watanabe, J. Wiórkiewicz-Kuczera, D. Yin, M. Karplus, All-atom empirical potential for molecular modeling and dynamics studies of proteins, J. Phys. Chem. B 102 (1998) 3586–3616.
[23] W.L. Jorgensen, J. Chandrasekhar, J.D. Madura, R.W. Impey, M.L. Klein, Comparison of simple potential functions for simulating liquid water, J. Chem. Phys. 79 (1982) 926–935.
[24] J.P. Ryckaert, G. Ciccotti, H.J.C. Berendsen, Numerical integration of the cartesian equations of motion of a system with constraints: molecular dynamics of *n*-alkanes, J. Comput. Phys. 23 (1977) 327–341.
[25] S. Miyamoto, P.A. Kollman, SETTLE: an analytical version of the SHAKE and RATTLE algorithm for rigid water models, J. Comput. Chem. 13 (1992) 952–962.
[26] G.J. Martyna, D.J. Tobias, M.L. Klein, Constant pressure molecular dynamics algorithms, J. Chem. Phys. 101 (1994) 4177–4189.
[27] T.W. Allen, O.S. Andersen, B. Roux, Energetics of ion conduction through the gramicidin channel, Proc. Natl. Acad. Sci. U. S. A. 101 (2004) 117–122.
[28] H.J. Woo, B. Roux, Calculation of absolute protein-ligand binding free energy from computer simulations, Proc. Natl. Acad. Sci. U. S. A. 102 (2005) 6825–6830.
[29] C.S. Park, C. Miller, Interaction of charybdotoxin with permeant ions inside the pore of a $K^+$ channel, Neuron 9 (1992) 307–313.
[30] Y. Kubo, J.P. Adelman, D.E. Clapham, L.Y. Jan, A. Karschin, Y. Kurachi, M. Lazdunski, C.G. Nichols, S. Seino, C.A. Vandenberg, International Union of Pharmacology. LIV. Nomenclature and molecular relationships of inwardly rectifying potassium channels, Pharmacol. Rev. 57 (2005) 509–526.
[31] Y. Ramu, A.M. Klem, Z. Lu, Short variable sequence acquired in evolution enables selective inhibition of various inward-rectifier $K^+$ channels, Biochemistry 43 (2004) 10701–10709.
[32] C.H. Yang, Paired interactions between Kir channels and Tertiapin-Q, Maters Thesis in Physiology, Virginia Commonwealth University, 2013.